Nanosecond reverse saturable absorption in cubanelike transition-metal clusters

W. Ji, H. J. Du, and S. H. Tang

Department of Physics, National University of Singapore, Lower Kent Ridge Road, Singapore

S. Shi

Optical Crystal Laboratory and Department of Chemical Engineering,
National University of Singapore, Kent Ridge Crescent, Singapore

We report the measurement of reverse saturable absorption in four cubanelike transition-metal clusters with nanosecond laser pulses. We also present a five-level rate-equation model in which ionization and germinate recombination are included. A comparison between the model and the measured data shows that the population of the triplet states is generated mainly through the ionization–recombination process, and triplet–triplet absorption is responsible for the measured reverse saturable absorption.

1. INTRODUCTION

For the past decade materials exhibiting strong nonlinear-optical properties have been studied intensively.[1] Interest in these materials has been stimulated not only by the quest for understanding of nonlinear-optical phenomena but also by their potential technological applications.[2] The currently rapid advances in the development of high-power frequency-agile lasers have led to a growing demand for optical limiting devices[3] designed to protect sensitive optical sensors from intense laser radiation. One can realize such devices by exploiting materials whose absorption is weak at low incident light energy but becomes extremely strong under intense light radiation. Such nonlinear absorptive behavior is referred as reverse saturable absorption (RSA), in contrast to saturable absorption found in most materials. We report here an experimental investigation of RSA effects in cubanelike transition-metal clusters with nanosecond laser pulses. A five-level rate-equation model is also presented to describe the responsible mechanism.

The RSA process was first observed by Giuliano and Hess[4] in dye molecules such as Sudanschwartz-B and Indanthrone. Since then a number of compounds have been found to possess such a property. These compounds include phthalocyanine,[5,6] metallophthalocyanine,[6,7] ion tricobalt clusters,[8] and King's complex.[9–11] Physically, RSA occurs as a consequence of the absorption cross section of an excited molecular state being greater than that of the ground state. As the optical excitation intensity increases, more molecules are promoted to the excited state, thus giving rise to higher absorption at intense light excitation. Because the RSA process involves electronic transitions, materials that exhibit RSA generally have an extremely fast response. Many examples of the RSA process involve a long-lived triplet state. This is certainly true when the samples are illuminated by light pulses of a few nanoseconds or longer. The involvement

of a long-lived triplet state ensures that the optical limiting response is relatively pulse-width independent over a wide range of pulse durations. Furthermore, many of these molecules have a broad linear absorption, resulting in a broadband limiting response. These advantages make RSA extremely attractive for use in broadband optical limiting of laser pulses.

In the past few years, fullerenes (C_{60}) have received a great deal of attention because this molecule also possesses strong RSA, which results in a low limiting threshold.[11–14] The RSA process in C_{60} can be described by a five-level (three singlet states and two triplet states) model. In particular, the triplet–triplet transition has been identified as the main mechanism responsible for nanosecond optical limiting.[13,14] However, McLean *et al.*[14] found that the five-level model in which the triplet states are populated through intersystem crossing can explain the limiting effect only to a fluence range of up to 1.5 J/cm². On the other hand, Abakumov *et al.*[15,16] reported that, under laser radiation, the population in the triplet states of organic molecules can be accumulated through another channel, that is, through a process of ionization and subsequently germinate recombination. In this process, incident light excites molecules from the ground state to the first excited singlet state, S_1. The excited molecules at the S_1 state are then ionized by absorbing photons; and the ions rapidly recombine to reform the molecules, some of which return to the S_1 state while the others end up at the first excited triplet state.

Recently we reported the observation of nanosecond optical limiting effects in four cubanelike transition metal clusters.[17,18] The molecular structures of these clusters, as shown in Fig. 1, are similar to a cubic cage with eight vertices alternately occupied by metal and nonmetal atoms and twelve edges representing metal–nonmetal bonds. The optical limiting performance of these new compounds has been experimentally shown to be better than that for C_{60}. In this
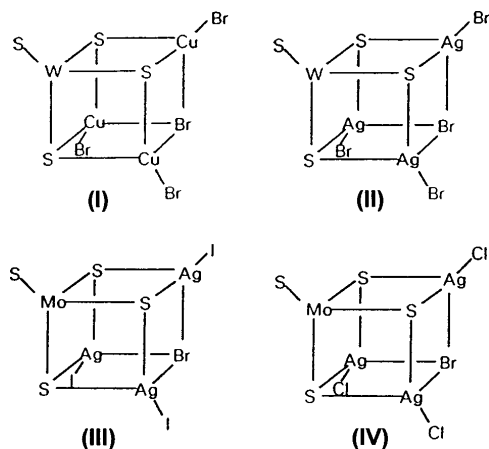
Fig. 1. Molecular structures of the clusters $(n\text{-}Bu_4N)_3$ $[WCu_3Br_4S_4]$ (compound I), $(n\text{-}Bu_4N)_3[WAg_3Br_4S_4]$ (compound II), $(n\text{-}Bu_4N)_3[MoAg_3BrI_3S_4]$ (compound III), and $(n\text{-}Bu_4N)_3$ $[MoAg_3BrCI_3S_4]$ (compound IV). After Refs. 17 and 18.

paper we present a study of RSA in these compounds by measuring the fluence-dependent transmittance with nanosecond laser pulses over a spectral range of visible light. Narrowing in the temporal profiles of the transmitted pulses is also reported. We propose a RSA model, which includes ionization and subsequently germinate recombination, to explain the observed RSA. By comparing the model simulation with the experimental data, we show that absorption transitions between the triplet states play an important role in the observed RSA and that the population of the triplet states is created mainly by the process of ionization and recombination. To our knowledge, this is the first report of such a process included in the interpretation of optical limiting behavior.

2. EXPERIMENT

A. Sample Preparation

The four compounds used for nonlinear transmission measurements were prepared according to published procedures.[17,18] Compound I $((n\text{-}Bu_4N)_3[WCu_3Br_4S_4])$ was synthesized by a solid-state reaction. A well-ground mixture of ammonium tetrathiotungstate $[(NH_4)_2WS_4$ (1.0 mmol)], copper(I) bromide [CuBr (4.0 mmol)], and tetrabutylammonium bromide $[(n\text{-}Bu)_4NBr$ (3.0 mmol)] was sealed in a reaction tube under argon. We obtained a dark solid by heating the mixture to 100 °C for 15 h. The black, solid raw product of the reaction was extracted by 60 mL of dichloromethane (CH_2Cl_2). Compound I was crystallized out from the CH_2Cl_2 extract after more than 80% of the solvent was slowly evaporated. Compound II $((n\text{-}Bu_4N)_3[WAg_3Br_4S_4])$ was synthesized according to the same procedure, except that copper(I) bromide was replaced by silver(I) bromide. Compound III $((n\text{-}Bu_4N)_3[MoAg_3BrI_3S_4])$ and compound IV $((n\text{-}Bu_4N)_3[MoAg_3BrCl_3S_4])$ were obtained by similar procedures, except that $(NH_4)_2WS_4$ (1.0 mmol) was replaced by $(NH_4)_2MoS_4$ (1.0 mmol) and CuBr and AgBr were replaced by AgI, and AgCl, respectively. The crystal structures of the compounds were determined by single-crystal x-ray diffraction data, and the absorption spectra were examined with a spectrophotometer (Hitachi

U-3410). The results are in excellent agreement with the previously published data.[17,18]

B. Optical Measurements

The compounds were dissolved in either acetonitrile (CH_3CN) or acetone (CH_3COCH_3) and contained in a 1-mm-thick quartz cuvette. Their optical responses were measured with linearly polarized optical pulses from a Q-switched frequency-doubled Nd:YAG laser or from a dye laser pumped by the Nd:YAG laser. The experimental setup used for nonlinear transmission measurements was similar to that described in Ref. 19. The spatial profiles of the optical pulses were nearly Gaussian after passing through a spatial filter. The laser pulses were focused onto the sample by a focusing mirror of 25-cm focal length. The spot radius of the laser pulses at the cuvette was 35 ± 5 μm (half-width of $1/e^2$ maximum in irradiance). Both incident and transmitted laser pulses were monitored simultaneously by a calibrated beam splitter and two energy detectors (Laser Precision, RjP-735 energy probes). The detectors were linked to a computer by an IEEE interface. To avoid nonlinear-optical effects such as self-focusing, self-defocusing, and nonlinear scattering, we placed the transmission detector just after the exit plane of the sample so that all the transmitted light was collected. We carefully checked for other possible contributing sources of these kinds of effects, such as induced scattering caused by the formation of bubbles at high incident fluences,[20] and found none under our experimental conditions (incident fluences < 5 J/cm^2).

The temporal profiles of the incident and the transmitted pulses were recorded simultaneously. We did this by replacing the two energy detectors by two fast-response photodetectors (Electro-Optics Technology ET2010, response time <1 ns). The signals of the photodetectors were displayed on a Tektronix 7104 oscilloscope and digitized by a CCD camera system.

3. RESULTS

Figure 2 displays the fluence-dependent transmittance of the four compounds for a wavelength of 532 nm. It can be seen immediately that the transmittance decreases as the incident fluence increases. Similar behavior has been observed at wavelengths up to 630 nm for compounds III and IV. We define the limiting threshold as the incident fluence at which the transmittance falls to 50% of the linear transmittance. Table 1 shows the measured limiting thresholds, indicating that compounds III and IV can be used as broadband optical limiters. The RSA responses of compounds I and II become weaker at wavelengths longer than 560 nm. This is consistent with the linear absorption spectra of these compounds, which show extremely small linear absorbance (<400 M^{-1}) in the range from 560 to 1000 nm.[17]

It has also been found that the temporal shapes of the transmitted pulses become narrower as the input fluence increases. All four of the compounds exhibit this phenomenon, a typical example of which is shown in Fig. 3. The narrowing of the transmitted pulse clearly indicates that the observed nonlinear absorption is an accumulat-
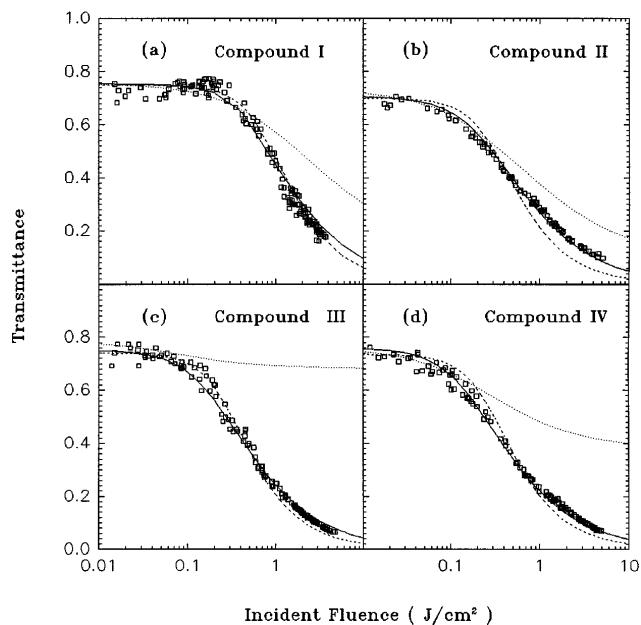
Fig. 2. Fluence-dependent transmittance of the compounds. The open squares are the data measured with 7-ns laser pulses of 532-nm wavelength. The curves are calculated by use of the five-level model described in the text.

Table 1. Experimentally Measured Limiting Thresholds of (n-Bu$_4$N)$_3$[MoAg$_3$BrI$_3$S$_4$] (Compound III) and (n-Bu$_4$N)$_3$[MoAg$_3$BrCl$_3$S$_4$] (Compound IV)

Compound	λ (nm)	F_{th} (J/cm^2)
III	532	0.5
	562	2.2
	570	2.2
	629	1.5
IV	532	0.6
	562	2.7
	570	2.3
	629	1.4

ing process that is an essential characteristic of an RSA process involving a long-lived excited state.

4. THEORY

To obtain more insight into the observed effects we developed a five-level rate-equation model. The molecular structures of the transition-metal clusters assume cubanelike structures and T_d symmetry. It is interesting to note that King's complex also possesses T_d symmetry. The molecular energy levels of King's complex were determined to belong to a set of singlet states and a set of triplet states.[21] Therefore it is reasonable for us to assume that the energy levels of the transition-metal clusters also consist of singlet states and triplet states. As we show in Section 5, it is necessary to include one ionized state in our model. Figure 4 illustrates all the energy levels involved in the RSA process of the transition-metal clusters.

The photodynamics of the system is described as follows. Initial absorption of the laser light promotes molecules from the ground state, S_0, to one of the manifold of vibrational–rotational states in the first excited

singlet state, S_1, which relax rapidly to the lowest level of this electronic state. Then some of the excited molecules are transferred to the first excited triplet state, T_1, by either intersystem crossing or a process of ionization and subsequently germinate recombination. In the latter process the molecules at state S_1 are ionized by light absorption to the ionized state; then the ionized molecules quickly recombine with electrons within the solvent cage and return partially to the T_1 state. Further absorption excites the molecules at state T_1 to a higher triplet state. If the absorption cross section of the T_1 state is greater than that of the ground state, the absorption becomes stronger as the incident fluence increases.

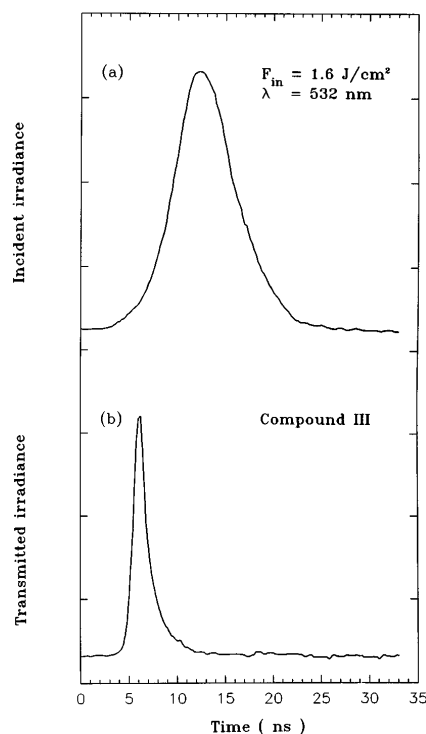The time derivatives of populations of states S_0, S_1, and

Fig. 3. Temporal profile of the incident and transmitted pulses for compound III. The wavelength and the incident fluence are 532 nm and 1.6 J/cm^2, respectively. Both the incident and the transmitted pulses are normalized to their peaks.
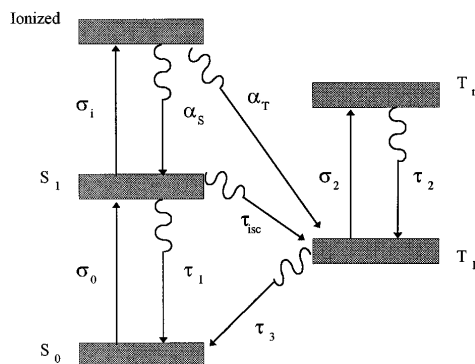

Fig. 4. Five-level model that describes reverse saturable absorption in the compounds. The wiggly-and-straight lines indicate the nonradiative decay, intersystem crossing, and germinate recombination processes. The straight lines indicate the absorption transition and ionization processes.

Table 2. Experimental Values of Ground-State Cross Section σ_0 and Limiting Threshold F_{in} and Theoretical Values of the Product of α_T, σ_i, σ_2, and τ_1

Compound	Formula	σ_0 (cm^2)[a]	F_{th} (J cm^{-2})[a]	$\alpha_T\sigma_i\sigma_2\tau_1$ (cm^4 ns)[b]
I	$(n\text{-Bu}_4\text{N})_3[\text{WCu}_3\text{Br}_4\text{S}_4]$	4.4×10^{-19}	1.1	1.0×10^{-35}
II	$(n\text{-Bu}_4\text{N})_3[\text{WAg}_3\text{Br}_4\text{S}_4]$	1.4×10^{-18}	0.6	8.5×10^{-35}
III	$(n\text{-Bu}_4\text{N})_3[\text{MoAg}_3\text{BrI}_3\text{S}_4]$	1.8×10^{-17}	0.5	9.6×10^{-35}
IV	$(n\text{-Bu}_4\text{N})_3[\text{MoAg}_3\text{BrCl}_3\text{S}_4]$	4.6×10^{-18}	0.6	1.0×10^{-34}

[a]These values were obtained from our experiment at a wavelength of 532 nm.
[b]These values were determined by the best fits between our theory and experimental data.

T_1 and the density of the ionized molecules (n_0, n_1, n_2, and n_3, respectively) are given by

$$\frac{\partial n_0}{\partial t} = \frac{n_1}{\tau_1} - \frac{\sigma_0 n_0}{h\nu}I, \qquad (1)$$

$$\frac{\partial n_1}{\partial t} = \frac{\sigma_0 n_0}{h\nu}I + \alpha_S k_e n_3{}^2 - \frac{n_1}{\tau_1} - \frac{n_1}{\tau_{isc}} - \frac{\sigma_i n_1}{h\nu}I, \qquad (2)$$

$$\frac{\partial n_2}{\partial t} = \frac{n_1}{\tau_{isc}} + \alpha_T k_e n_3{}^2, \qquad (3)$$

$$\frac{\partial n_3}{\partial t} = \frac{\sigma_i n_1}{h\nu}I - (\alpha_S + \alpha_T)k_e n_3{}^2, \qquad (4)$$

where σ_0 is the absorption cross section of the S_0 state; σ_i is the cross section for the ionization; τ_1 and τ_{isc} are the relaxation time of the S_1 state and the intersystem crossing time, respectively; k_e is the coefficient of cation–electron recombination; α_S and α_T are the probabilities of reforming the molecules in the S_1 and T_1 states, respectively; I is the irradiance of the light pulse; h is the Planck constant; and ν is the frequency of light.

The propagation of the light pulse is determined by the wave equation. Taking a slowly varying envelope approximation we may write it as

$$\frac{\partial I}{\partial z} = -(n_0\sigma_0 + n_1\sigma_i + n_2\sigma_2)I, \qquad (5)$$

where z is the propagation distance in the sample and σ_2 is the absorption cross section of the T_1 state.

In Eqs. (1)–(5), stimulated emissions from the excited states are neglected. The probability of re-forming the molecules in the ground state by germinate recombination is so small that it is also ignored.[16] It is assumed that the relaxation time (τ_2) from the higher excited triplet state, T_n, is fast enough that the T_1 state is not depopulated by light absorption. This assumption results in the disappearance of the absorption and relaxation terms between the T_1 and T_n states in Eq. (3). The relaxation time (τ_3) of the T_1 state to the ground state has been measured to be of the order of a few milliseconds.[18] It is too long in comparison with the duration of the laser pulse; hence it is excluded from Eqs. (1) and (3). The solution of Eqs. (1)–(5) was obtained numerically by use of Gaussian-shaped temporal and spatial profiles of the incident laser pulse. The numerical solution was then integrated over time and space to produce an energy transmittance as a function of the incident fluence that could be compared with the experimental data. The calculated results for the four cluster compounds at 532 nm are displayed in Fig. 2.

5. DISCUSSION

The values of the ground-state cross section σ_0 at 532 nm used in the calculation were obtained from the experiments and are listed in Table 2. It was reported that the ratio of α_S and α_T is ~3:1 and that the germinate recombination coefficient is of the order of 10^{12} M^{-1} s^{-1}.[22] We adopt these values for our transition-metal clusters. Our numerical calculations show that varying these two quantities in the ranges from 1:9 to 9:1 and from 5×10^{11} to 5×10^{13} M^{-1} s^{-1}, respectively, has little effect on the following conclusions. No measurements of other photophysical parameters (σ_2, σ_i, τ_1, and τ_{isc}) have been reported to our knowledge. They were treated as adjustable parameters in our numerical calculations. The results are shown by the solid curves in Fig. 2. It is obvious that the model can predict the limiting behavior. Note that we achieved the good agreement by using a set of the adjustable parameters, which has led to an uncertainty in the quantitative description of the limiting mechanism. However, the model simulation does give the following two qualitative conclusions:

(a) Inclusion of excited-triplet-state absorption is essential. We confirmed this by performing the calculations with a fixed value for $\sigma_2 = 0$ and adjusting the other parameters (σ_i, τ_{isc}, and τ_1) systematically from very small values to very large values. Examples of such calculations are represented by the dotted curves in Fig. 2, which fit the experimental data well in the low-energy range (<0.2 J/cm^2). But the significant discrepancy at higher energies implies that excited-state absorption, excluding triplet–triplet transitions, cannot explain the observed limiting effect. This is consistent with the observation in C_{60} under excitation of nanosecond laser pulses.[13,14]

(b) As we stated above, the model requires an ionization–recombination channel to populate the T_1 state efficiently. We have found that the model completely fails if this transfer channel is switched off. We obtained this conclusion by conducting similar calculations, except that α_T was set to be zero.

The best fits between the model and the experimental data as shown in Fig. 2 generate a set of values for the parameters σ_2, σ_i, τ_1, and τ_{isc}. With these values we calculated the population of the T_1 state as a function of time. Figure 5 illustrates such an example, showing the calculated generation rate of the T_1 state population created by the intersystem crossing (the dashed curve) and that generated by the ionization–recombination process (the solid curve). It is clear that the population
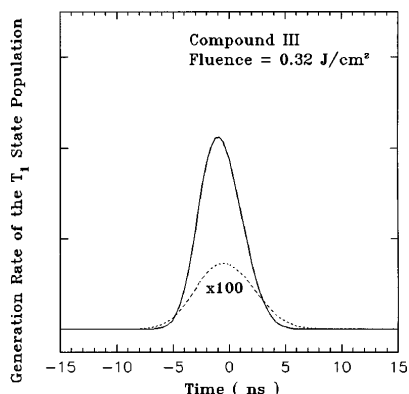
Fig. 5. Generation rate of the T_1 state population in compound III as a function of time. It is normalized to the peak of the generation rate of the T_1 state population by the ionization–recombination process. The solid curve shows the population of state T_1 created by the ionization–recombination process. The dashed curve shows the population of state T_1 generated by the intersystem crossing magnified 100×.

of the T_1 state is generated predominantly by the ionization–recombination process, and the intersystem crossing can be neglected. With this approximation, Eqs. (1)–(5) may be simplified to

$$\frac{\partial I}{\partial z} = -\sigma_0 n I \left[1 + \frac{\alpha_T \sigma_i \sigma_2 \tau_1}{(h\nu)^2} \int_{-\infty}^{t} I^2(t') \mathrm{d}t' \right], \qquad (6)$$

where n is the total molecule concentration. Integrating Eq. (6) over time, we obtain

$$\frac{\mathrm{d}F}{\mathrm{d}z} = -\sigma_0 n F(1 + BF^2), \qquad (7)$$

where F is the fluence inside the sample, $B = \alpha_T \sigma_i \sigma_2 \tau_1 / [2\sqrt{2\pi} t_p (h\nu)^2]$, and t_p is the half-width at e^{-1} maximum of the pulse duration. Considering the surface reflectance of the sample, we can obtain the fluence-dependent transmittance as follows:

$$T = \frac{(1 - R)^2 \exp(-\sigma_0 n L)}{\{1 + B[1 - \exp(-2\sigma_0 n L)]F_{\mathrm{in}}^2\}^{1/2}}, \qquad (8)$$

where L is the thickness of the sample, R is the surface reflectance of the sample, and F_{in} is the incident fluence. Equation (8) clearly shows that the product of quantities α_T, σ_i, σ_2, and τ_1 dictates the optical limiting performance. The larger these quantities are, the stronger the RSA response is. It also demonstrates that the RSA is caused by the absorption transitions of the triplet state whose population is created by the ionization–recombination process. The dashed curves in Fig. 2 are calculated by Eq. (8) and are in good agreement with the experimental data. Table 2 summarizes the product of α_T, σ_i, σ_2, and τ_1 obtained from the best fits between the numerical results of Eq. (8) and the measured data.

It is interesting to note that intersystem crossing is a dominant process for creating population in the triplet state of C_{60} molecules[13,14] and phthalocyanine derivatives.[5,7] Our cluster compounds are notably different from these RSA molecules in containing many ionizable low-valence IB elements and chalcogenide. Perhaps

more importantly, the optical limiting performance of our compounds was observed in acetonitrile, whereas the nonlinear transmission measurements of both C_{60} and phthalocyanine derivatives were conducted in toluene.[5,7,13,14] Acetonitrile is a much more polar solvent than toluene and is capable of facilitating an ionization process.

6. CONCLUSION

We have measured reverse saturable absorption in four cubanelike transition-metal clusters with nanosecond laser pulses. The measured results show that the compounds $(n\text{-}Bu_4N)_3[MoAg_3BrI_3S_4]$ and $(n\text{-}Bu_4N)_3[MoAg_3BrCl_3S_4]$ may be used as broadband optical limiters. We have also developed a five-level (two singlet states, two triplet states, and one ionized state) model that includes ionization and germinate recombination. A comparison of the model simulation with the experimental data shows that the triplet states are populated mainly through the ionization and germinate recombination in the clusters. It also shows that the triplet–triplet transitions are responsible for reverse saturable absorption.

REFERENCES

1. See, for example, D. S. Chemla and J. Zyss, eds., *Nonlinear Optical Properties of Organic Molecules and Crystals* (Academic, Orlando, Fla., 1987); R. A. Hann and D. Bloor, eds., *Organic Materials for Nonlinear Optics* (Royal Society of Chemistry, London, 1989); M. F. Kajzar, P. Prasad, and D. Ulrich, eds., *Nonlinear Optical Effects in Organic Polymers*, Vol. 162 of NATO ASI Series E (Kluwer, Dordrecht, The Netherlands, 1989).
2. See, for example, S. D. Smith, "Lasers, nonlinear optics and the optical computers: the first all-optical circuits," Nature (London) **316,** 319 (1985); B. S. Wherrett, A. C. Walker, and F. A. P. Tooley, "Nonlinear refraction for cw optical bistability," in *Optical Nonlinearities and Instabilities in Semiconductors*, H. Haug, ed. (Academic, Boston, Mass., 1988), pp. 239–272.
3. See, for example, R. C. C. Leite, S. P. S. Porto, and T. C. Damen, "The thermal lens effect as a power-limiting device," Appl. Phys. Lett. **10,** 100 (1967); M. J. Soileau, W. E. Williams, and E. W. Van Strayland, "Optical power limiter with picosecond response time," IEEE J. Quantum Electron. **QE-19,** 731 (1983); E. W. Van Stryland, Y. Y. Wu, D. J. Hagan, M. J. Soileau, and K. Mansour, "Optical limiting with semiconductors," J. Opt. Soc. Am. B **5,** 1980 (1988).
4. C. R. Giuliano and L. D. Hess, "Nonlinear absorption of light: optical saturation of electronic transitions in organic molecules with high intensity laser radiation," IEEE J. Quantum Electron. **QE-3,** 358 (1967).
5. T. H. Wei, D. J. Hagan, M. J. Sence, E. W. Van Stryland, J. W. Perry, and D. R. Coulter, "Direct measurements of nonlinear absorption and refraction of phthalocyanines," Appl. Phys. B **54,** 46 (1992).
6. D. J. Hagan, T. Xia, A. A. Said, T. H. Wei, and E. W. Van Stryland, "High dynamic range passive optical limiters," Intl. J. Nonlin. Opt. Phys. **2,** 483 (1993).
7. J. W. Perry, K. Mansour, S. R. Marder, K. J. Perry, D.

Alvarez, and I. Choong, "Enhanced reverse saturable absorption and optical limiting in heavy-atom substituted phthalocyanines," Opt. Lett. **19,** 625 (1994).

8. L. W. Tutt and S. W. McCahon, "Reverse saturable absorption in metal cluster compounds," Opt. Lett. **15,** 700 (1990).

9. G. R. Allan, D. R. Labergerie, S. J. Rychnovsky, T. F. Boggess, A. L. Smirl, and L. Tutt, "Picosecond reverse saturable absorption in King's complex [(C$_5$H$_5$Fe(CO)]$_4$]," J. Phys. Chem. **96,** 6313 (1992).

10. T. F. Boggess, G. R. Allan, S. J. Rychnovsky, D. R. Labergerie, C. H. Venzke, A. L. Smirl, L. W. Tutt, A. R. Kost, S. W. McCahon, and M. B. Klein, "Picosecond investigations of optical limiting mechanisms in King's complex," Opt. Eng. **32,** 1063 (1993).

11. A. Kost, L. Tutt, M. B. Klein, T. K. Dougherty, and W. E. Elias, "Optical limiting with C$_{60}$ in poly(methyl methacrylate)," Opt. Lett. **18,** 334 (1993).

12. L. W. Tutt and A. Kost, "Optical limiting performance of C$_{60}$ and C$_{70}$ solutions," Nature (London) **356,** 225 (1992).

13. F. Henari, J. Callaghan, H. Stiel, W. Blau, and D. J. Cardin, "Intensity-dependent absorption and resonant optical nonlinearity of C$_{60}$ and C$_{70}$ solution," Chem. Phys. Lett. **199,** 144 (1992).

14. D. G. McLean, R. L. Sutherland, M. C. Brant, D. M. Brandelik, P. A. Fleitz, and T. Pottenger, "Nonlinear absorption study in a C$_{60}$-toluene solution," Opt. Lett. **18,** 858 (1993).

15. G. A. Abakumov, B. I. Polyakov, A. P. Simonov, and T. M. Skavinskaya, "Fluorescence of complex organic molecules in a buffer gas during intense optical excitation," Opt. Spectrosc. (USSR) **74,** 641 (1993).

16. G. A. Abakumov, V. B. Koloxsky, B. I. Polyakov, and A. P. Simonov, "Germinate and volume electron-cation recombination in a polyatomic buffer gas," Chem. Phys. Lett. **182,** 321 (1992).

17. S. Shi, W. Ji, J. P. Lang, and X. Q. Xin, "New nonlinear optical chromophore: synthesis, structure, and optical limiting effect of transition-metal clusters $(n\text{-Bu}_4\text{N})_3[\text{W}M_3\text{Br}_4\text{S}_4]$ (M = Cu and Ag)," J. Phys. Chem. **98,** 3570 (1994).

18. S. Shi, W. Ji, S. H. Tang, J. P. Lang, and X. Q. Xin, "Synthesis and optical limiting capability of cubane-like mixed metal clusters $(n\text{-Bu}_4\text{N})_3[\text{MoAg}_3\text{Br}X_3\text{S}_4]$ (X = Cl and I)," J. Am. Chem. Soc. **116,** 3615 (1994).

19. W. Ji, S. H. Tang, and A. K. Kukaswadia, "Self-defocusing in GaP induced by band-gap resonant nonlinear refraction," J. Appl. Phys. **73,** 8455 (1993).

20. K. Mansour, M. J. Soileau, and E. W. Van Stryland, "Nonlinear optical properties of carbon-black suspensions (ink)," J. Opt. Soc. Am. B **9,** 1100 (1994).

21. Trinh-Toan, W. P. Fehlhammer, and L. F. Dahl, "Structure and bonding of the tetrameric cyclopentadienyliron carbonyl monocation, $[\text{Fe}_4(h^5\text{-C}_5\text{H}_5)_4(\text{CO})_4]^+$. Stereo chemical effect due to oxidation of a completely bonding tetrahedral metal cluster system," J. Am. Chem. Soc. **94,** 3389 (1972).

22. See, for example, J. B. Birks, *Photophysics in Aromatic Molecules* (Wiley-Interscience, New York, 1970), p. 398.